2015

Assessing Phosphine–Chalcogen Bond Energetics from Calculations

Samuel R. Alvarado
Iowa State University

Ian A. Shortt
Prairie View A & M University

Hua-Jun Fan
Prairie View A & M University

Javier Vela
Iowa State University

Assessing Phosphine–Chalcogen Bond Energetics from Calculations

Abstract
Phosphine chalcogenides are useful reagents in chalcogen atom transfer reactions and nanocrystal syntheses. Understanding the strength and electronic structure of these bonds is key to optimizing their use, but a limited number of experimental and computational studies probe these issues. Using density functional theory (DFT), we computationally screen multiple series of trisubstituted phosphine chalcogenide molecules with a variety of phosphorus substituents and examine how these affect the strength of the phosphorus-chalcogen bond. DFT provides valuable data on these compounds including P-E bond dissociation energies, P-E bond order,Löwdin charge on phosphorus and chalcogen atoms, and molecular geometries. Experimentally monitoring the ^{31}P and ^{77}Se NMR chemical shifts and published Hammett constants provides good estimates and confirmation of the relative magnitude of electronic shielding around these nuclei and confirms the predictive value of the computational results.

Keywords
chalcogenides, chemical bonds, computation theory, electronic structure, inorganic compounds, phosphorus, bond dissociation energies, computational results, Hammett constants, molecular geometries, nanocrystal synthesis, NMR chemical shifts, phosphine chalcogenides, density functional theory

Disciplines
Chemistry | Inorganic Chemistry

Comments
Reprinted (adapted) with permission from *Organometallics* 34 (2015): 4023, doi: 10.1021/acs.organomet.5b00428.

ORGANOMETALLICS

Article

pubs.acs.org/Organometallics

Assessing Phosphine−Chalcogen Bond Energetics from Calculations

Samuel R. Alvarado,[†,‡] Ian A. Shortt,[§] Hua-Jun Fan,[*,§] and Javier Vela[*,†,‡]

[†]Department of Chemistry, Iowa State University, Ames, Iowa 50011, United States

[‡]Ames Laboratory, Ames, Iowa 50011, United States

[§]Department of Chemistry, Prairie View A&M University, Prairie View, Texas 77446, United States

Supporting Information

ABSTRACT: Phosphine chalcogenides are useful reagents in chalcogen atom transfer reactions and nanocrystal syntheses. Understanding the strength and electronic structure of these bonds is key to optimizing their use, but a limited number of experimental and computational studies probe these issues. Using density functional theory (DFT), we computationally screen multiple series of trisubstituted phosphine chalcogenide molecules with a variety of phosphorus substituents and examine how these affect the strength of the phosphorus−chalcogen bond. DFT provides valuable data on these compounds including P−E bond dissociation energies, P−E bond order, Löwdin charge on phosphorus and chalcogen atoms, and molecular geometries. Experimentally monitoring the ^{31}P and ^{77}Se NMR chemical shifts and published Hammett constants provides good estimates and confirmation of the relative magnitude of electronic shielding around these nuclei and confirms the predictive value of the computational results.

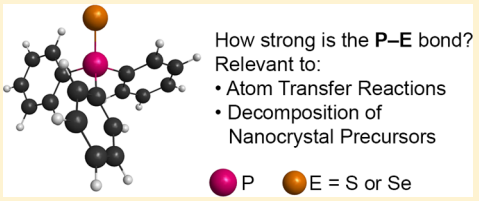

INTRODUCTION

Tertiary (trisubstituted) phosphine chalcogenides (R_3PE, where R = alkyl, aryl, amide, alkoxyl, and E = S, Se, Te) are molecular compounds useful in a variety of chemical transformations including chalcogen atom transfer reactions and chalcogenide nanocrystal synthesis. In comparison to the unsupported elemental chalcogens, the substituents (R) on the phosphine chalcogenide can be used to fine-tune the solubility and reactivity of the phosphorus−chalcogen (PE) moiety in these compounds.[1]

In atom transfer reactions, phosphine chalcogenides donate sulfur, selenium, or tellurium in a bimolecular fashion.[2,3] Current evidence indicates that the rate of atom transfer is dependent on the relative basicity of the pnictogen center (P, As, or Sb). This transfer can occur between a phosphine chalcogenide and another P, As, or Sb atom.[4] Computations suggest that the transfer of S and Se atoms among phosphines proceeds through chalcogen-philic attack by the pnictide nucleophile.[5] Phosphine sulfide-supported palladium complexes[6] as well as Cu(I) and Zn(II) catalysts[7] mediate this transformation. A synthetic application of this strategy is Se atom transfer from triphenylphosphine selenide to H-phosphonate diesters.[8] Similarly, tricyclohexylphosphine selenide and telluride donate a chalcogen atom to *N*-heterocyclic carbenes.[9]

Because of their desirable reactivity and solubility in low-volatility (high boiling point) solvents, trialkyl phosphine chalcogenides have been popular chalcogen sources in nanocrystal preparations since the early 1990s.[10] Cleavage of the P−E bond is thought to occur by either redox chalcogen (E^0) atom transfer or acid−base chalcogenide (E^{2-}) transfer mechanisms.[11] The latter mechanism proceeds through a phosphine chalcogenide-metal activated complex, which decomposes into metal chalcogenide nuclei.[12] The mechanism of R_3PE decomposition has been studied for the synthesis of CdSe,[13−15] PbSe,[16,17] and ZnSe[18] nanocrystals. The electron-donating and -withdrawing effects of different phosphorus substituents have an effect on the mechanism of InP formation from triarylsilylphosphines.[19]

Studies on the electronic structure of R_3PE compounds and the reactive P−E bond are key to guiding their use as both atom transfer reagents and nanocrystal synthesis precursors. It is well established that heavier chalcogens form significantly weaker and longer bonds with phosphorus. Calorimetric methods and atom transfer reactions have been used to measure the strength of P−E bonds experimentally.[20] Bond dissociation energies of phosphine sulfides spanned a range of 88−98 kcal/mol, while those of phosphine selenides were in the range 67−75 kcal/mol.[21] Bonding in trialkyl phoosphine chalcogenides[22,23] has also been studied computationally using density functional theory (DFT)[24] and atoms in molecules (AIM).[25] Our group recently used DFT to estimate the P−E bond strengths of a selection of phosphine sulfide and selenide derivatives that are particularly useful in the preparation of colloidal semiconductor nanocrystals (quantum dots and rods).[26]

Here we greatly expand our investigation of P−S and P−Se bond dissociation energies (BDEs) using DFT methods. To understand how changing the electron density around the PE moiety influences the electronic structure and strength of the P−E bond, we closely examine different families of

Received: May 20, 2015
Published: August 10, 2015

DOI: 10.1021/acs.organomet.5b00428
Organometallics 2015, 34, 4023−4031

Chart 1. Tertiary (Trisubstituted) Phosphine Chalcogenide Compounds (R_3PE, E = S or Se) Studied in This Work[a]

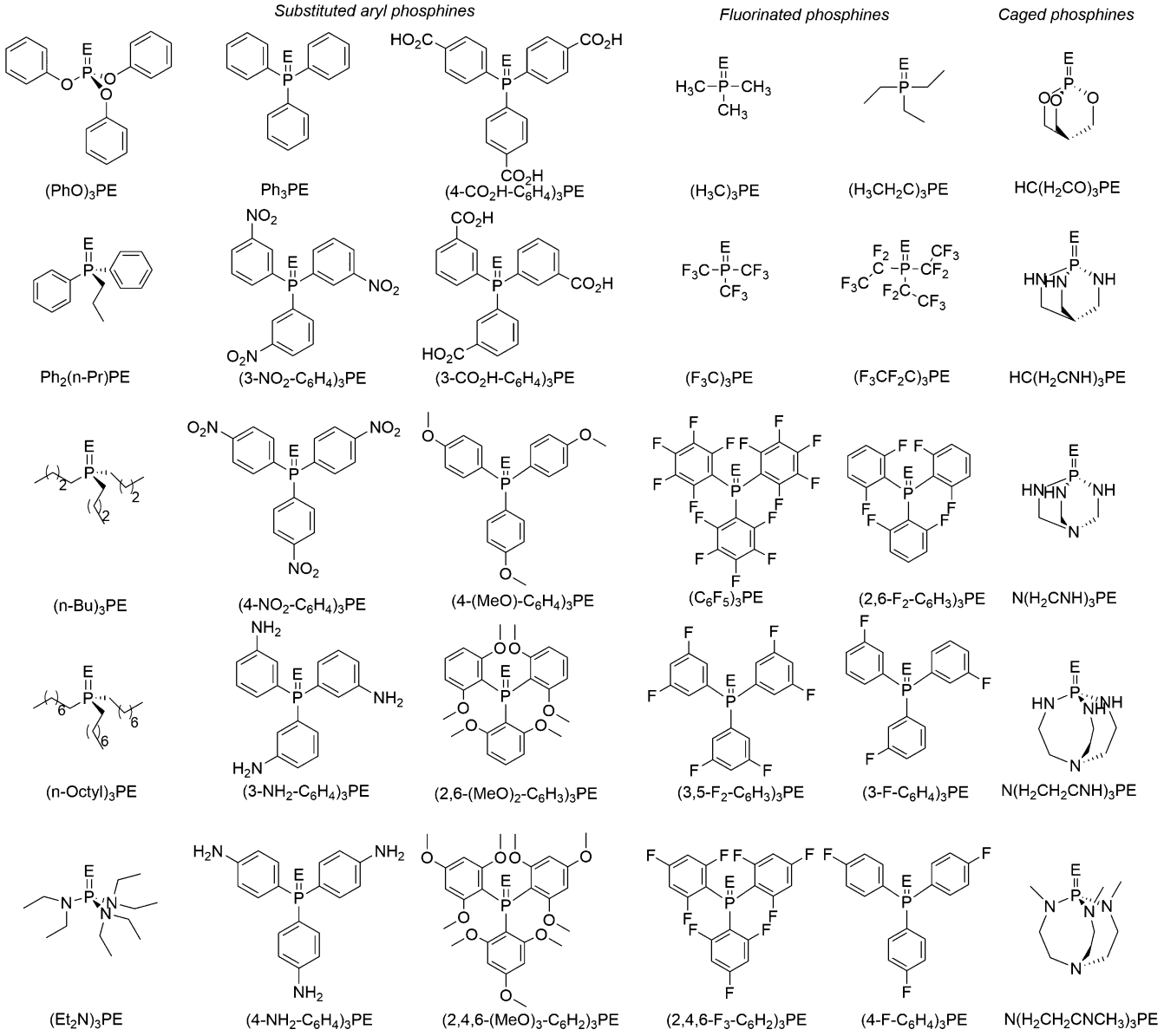

[a]The compounds in the first column were calculated previously.[26]

triarylphosphine chalcogenides containing substituents of varying resonance and inductive effects. We also investigate trialkyl, tris-perfluoroalkyl, and caged (Verkade-type) phosphine chalcogenides.[27] We anticipate that the results of this large computational screening will be generally applicable to a variety of problems and applications that make use of phosphine chalcogenides, including chalcogen atom transfer and nanomaterial synthesis reactions.

RESULTS AND DISCUSSION

We have previously shown that bond dissociation energies can be good indicators of molecular precursor reactivity and selectivity. Specifically, we have been able to use computed BDEs of tertiary phosphine chalcogenides[26] and disubstituted dichalcogenides[28] to predictably fine-tune the composition, aspect ratio (of rods), and morphology (from dots to rods to tetrapods) of CdS−CdSe nanocrystals. In the case of tertiary phosphine chalcogenides, 10 computed BDEs (five sulfides and five selenides) were correlated to experimental ^{31}P (and ^{77}Se NMR) data. Experiments showed that the relative rate of (homogeneous) CdE nucleation increases more dramatically than the rate of CdE growth (heterogeneous nucleation) with a decrease in precursor P−E bond energy (E = S or Se).[26]

In order to generalize this approach, we have used DFT (see Computational and Experimental Methods) to expand the range of computed tertiary phosphine chalcogenide BDEs. For simplicity, we categorize the specific chalcogenide compounds in our study into five families based on the type of tertiary phosphine that they are derived from: (a) triaryl phosphines monosubstituted with electron-donating or -withdrawing groups (amino, $-NH_2$; methoxy, −OMe; fluoro, −F; carboxyl, $-CO_2H$; nitro, $-NO_2$); (b) triaryl phosphines substituted with one, two, or three methoxy groups; (c) triaryl phosphines substituted with one, two, or three fluorines; (d) trialkyl and triperfluoroalkyl phosphines; and (e) caged (Verkade-type) tertiary phosphines (Chart 1).[27] In all cases, we modeled a

DOI: 10.1021/acs.organomet.5b00428
Organometallics 2015, 34, 4023−4031

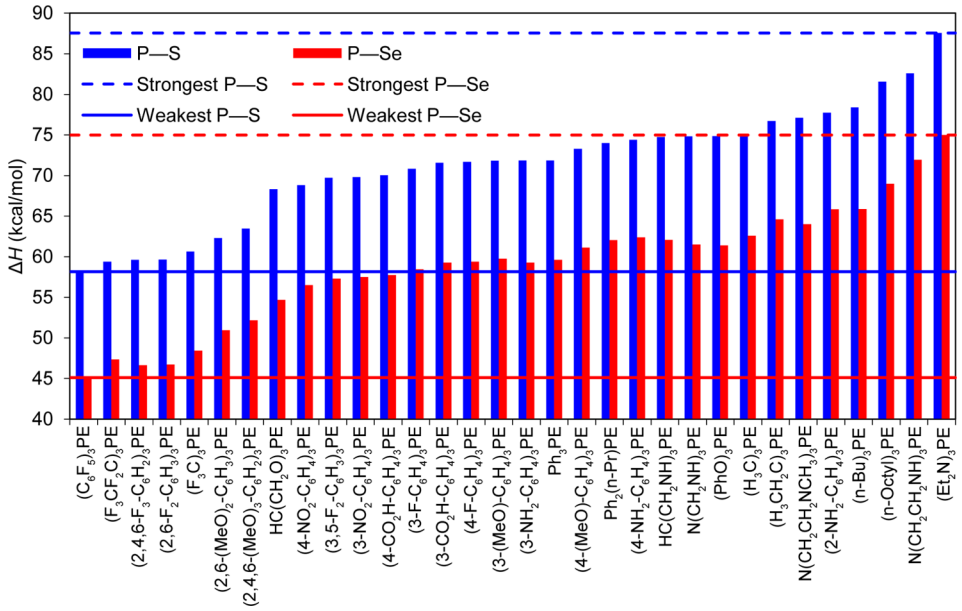

Figure 1. Calculated P−E bond dissociation enthalpies (ΔH) in tertiary phosphine sulfides (R_3PS) and selenides (R_3PSe). For consistency with prior work and discussions, we arbitrarily use values of ΔH as a measure of the P−E BDEs.

homolytic P−E bond dissociation energy for the release of sulfur or selenium atom from the corresponding phosphine chalcogenide. In all cases, we first optimized the geometries of R_3PE and R_3P, assumed triplet E, and calculated the change in electronic energy after correcting for zero-point energy (ΔE_{ZPE}), the change in enthalpy (ΔH), and the change in Gibbs free energy (ΔG) values corrected to 298.15 K (a full list of all of our results is available in the Supporting Information). For consistency with prior work and discussions, we arbitrarily use values of ΔH as a measure of the P—E BDEs (for trisubstituted phosphine chalcogenides calculated here and elsewhere, we find that the ΔH and ΔG values follow very similar trends).[26]

General Observations: Bond Strength vs Bond Length. Figure 1 shows the calculated BDEs (ΔHs) for all the compounds we have studied. Across the five compound families (a through e above), the heavier phosphine selenides exhibit significantly longer (by ca. 0.15 Å) and weaker (by ca. 13−15 kcal/mol) bonds compared to the corresponding phosphine sulfides (Figure 2). This is expected given that the larger selenium atom has larger, more diffuse orbitals, resulting in poorer orbital overlap with the phosphorus orbitals as compared to the smaller sulfur atom. Interestingly, this is not the case within each of the sulfide or selenide series, where the BDE actually increases with increasing P−E distance (with some exceptions, see below). For example, the monosubstituted triarylphosphine chalcogenides show a near-linear increase in BDE across the P−S and P−Se series individually (Figure 2a). This trend is also seen in fluorinated triaryl phosphines substituted with one, two, or three fluorines (Figure 2c), trialkyl and triperfluoroalkyl phosphines (Figure 2d), and caged Verkade phosphines (Figure 2e), although these are not as linear as the aromatic phosphine chalcogenides. While this trend was unexpected and may seem counterintuitive, there are several well-documented examples of longer bonds being stronger in covalent compounds of tin[29] and its lighter analogues,[30] as well as S−F bonds in SF_2 dimers.[31] A crystallographic study of phosphine adducts of open titanocenes also shows a similar correlation between bond strength and bond length.[32]

The only exception to the aforementioned trend comes from discontinuities in bond strengths and lengths observed for the methoxy- and, to a lesser extent, fluorine-substituted triarylphosphine chalcogenides (Figure 2b and c, respectively). The specific outliers are compounds that feature substitution at the 2 or *ortho* position, i.e., adjacent to the P−E bond, such as $(2,6\text{-}MeO_2\text{-}C_6H_3)_3PE$ (Chart 1). A possible explanation is that p orbitals from the adjacent heteroatom substituents (O, F) may be interacting with the P−E bond itself. This interaction could potentially increase the P−E distance and weaken the bond accordingly. To further investigate the presence and effect of this interaction, we visualized the total electron density of three molecules: Ph_3PS, $(2,6\text{-}(MeO)_2\text{-}C_6H_3)_3PS$, and $(C_6F_5)_3PS$ (Figure 3a−c). In the optimized geometries of the latter two compounds, electron density from the neighboring *ortho* substituents may interact with the P−E bond. Therefore, while the methoxy groups should increase electron density at the P−E bond via resonance effects—the reported pK_a of $(2,4,6\text{-}(MeO)_3\text{-}C_6H_2)_3PS$ is 11.2[33]—their steric bulk may actually cause significant weakening of the P−E bond. Calculated average distances for these interactions in $(2,6\text{-}(MeO)_2\text{-}C_6H_3)_3PS$, $(2,4,6\text{-}(MeO)_3\text{-}C_6H_2)_3PS$, $(2,6\text{-}(MeO)_2\text{-}C_6H_3)_3PSe$, and $(2,4,6\text{-}(MeO)_3\text{-}C_6H_2)_3PSe$ are 3.15, 3.16, 3.23, and 3.24 Å, respectively. Interestingly, in $(C_6F_5)_3PE$, one of the three aryl rings in these compounds is rotated nearly coplanar with the P−E bond (Figure 3c). The nearest calculated F−E interaction is 3.09 Å in $(C_6F_5)_3PS$ and 3.17 Å in $(C_6F_5)_3PSe$. The van der Waals radii of F, S, Se, and P are 1.47, 1.80, 1.90, and 1.80 Å, respectively.[34] Interactions between S and F atoms were previously revealed by single-crystal X-ray crystallography.[35,36]

Bond Strength vs Löwdin Charges. To understand why longer bonds are slightly stronger among homologous (chalcogen constant) families of phosphine chalcogenides, we examined the partial charge on the phosphorus and chalcogen atoms in these compounds using a Mülliken population analysis[37−40] of symmetrically orthogonalized orbitals.[41]

DOI: 10.1021/acs.organomet.5b00428
Organometallics 2015, 34, 4023−4031

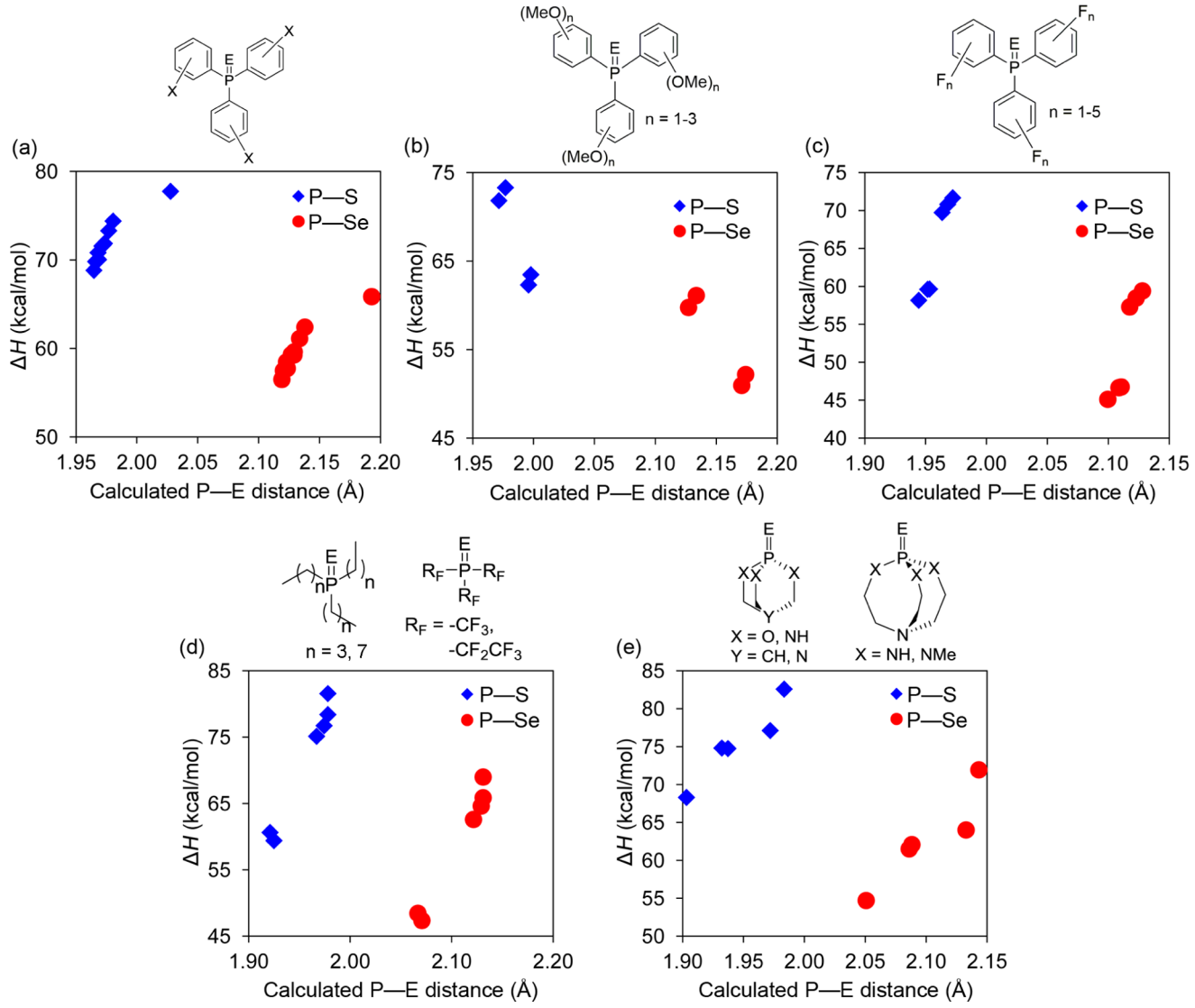

Figure 2. Calculated P−E bond dissociation enthalpies (ΔH) (E = S or Se) vs P−E distances for monosubstituted triarylphosphine chalcogenides (a), fluorinated triarylphosphine chalcogenides (b), methoxy-substituted triarylphosphine chalcogenides (c), trialkyl and triperfluoroalkyl phosphine chalcogenides (d), and caged (Verkade-type) tertiary phosphine chalcogenides (e).

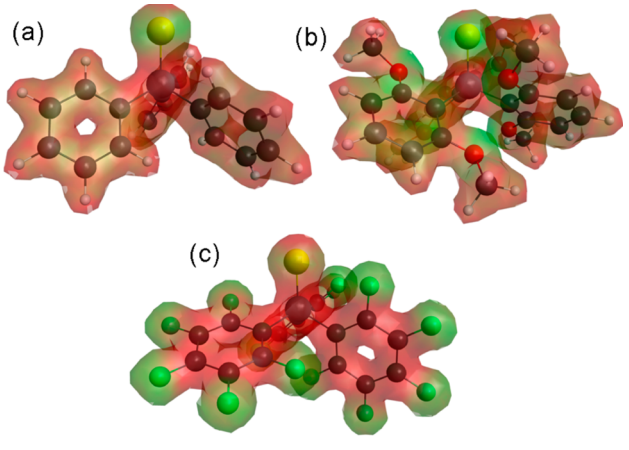

Figure 3. Total electron density, visualized at a contour value of 0.05, for Ph_3PS (a), $(2,6\text{-}MeO_2\text{-}C_6H_3)_3PS$ (b), and $(C_6F_5)_3PS$ (c). We note the close contact of p orbitals from methoxy groups to the P−E moiety.

Mülliken population analysis assigns a partial charge to each atom in the molecule. Subsequent Löwdin analysis prevents excessive charge buildup on any given atom, which in some cases can lead to more than two electrons sharing a single orbital.

Our Löwdin analysis clearly shows that the P atom is much more positively charged (by ca. 0.11+) in the R_3PSe compounds than in the analogous R_3PS compounds (Figure 4). Similarly, the chalcogen (E) atom is much more negatively charged (by ca. 0.10+) on the R_3PSe compounds than in the R_3PS compounds (Figure 4). Interestingly, in most compounds studied, a larger positive charge on P and a larger negative charge on E leads to an increase in the P−E BDE. This is true across chalcogens as well as within each separate (sulfide or selenide) family. Small deviations from this trend in the methoxy- and fluorine-*ortho*-substituted cases can be attributed to a redistribution of electron density around the P−E moiety due to close steric contacts as shown above (Figure 3).

The observation that a more positively charged P atom and a more negatively charged E atom result in a stronger P−E bonds

DOI: 10.1021/acs.organomet.5b00428
Organometallics 2015, 34, 4023−4031

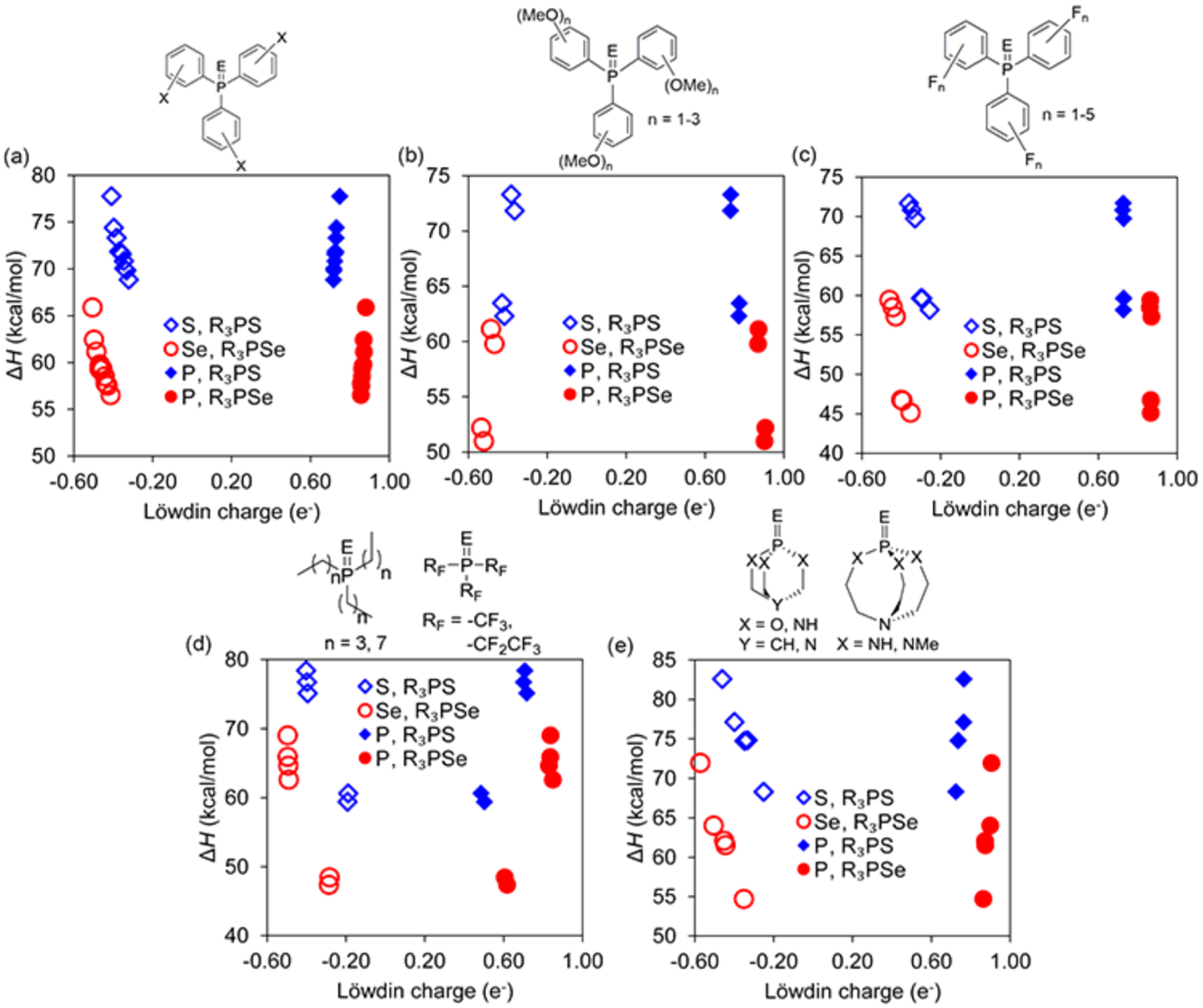

Figure 4. Calculated P−E bond dissociation enthalpies (ΔH) (E = S or Se) vs Löwdin charges on P and E atoms in monosubstituted triarylphosphine chalcogenides (a), fluorinated triarylphosphine chalcogenides (b), methoxy-substitued triarylphosphine chalcogenides (c), trialkyl and triperfluoroalkyl phosphine chalcogenides (d), and caged (Verkade-type) tertiary phosphine chalcogenides (e).

implies that, *in R_3PE compounds, the P−E bond strength increases with ionic character*. Three possible structures may be envisioned to rationalize the distribution of electron density around the P−E moiety in these compounds (Scheme 1). Structure I is a resonance form that features a double bond between formally neutral P and E atoms. Structure II is a zwitterionic resonance form that has a single bond between a positively charged P atom and a negatively charged E atom. Structure III is an intermediate between the first two resonance structures, containing some partial double-bond character and some partial charge on each P and E (Scheme 1). In line with previous investigations,[25] our results above strongly suggest that the P−E bond has an order between 1 and 2, is composed of a mixture of covalent and ionic character, and becomes stronger as the ionic character increases.

Scheme 1. Three Resonance Structures to Rationalize the Distribution of Electron Density around the P−E Bond in Tertiary Phosphine Chalcogenides: A Formal Double Bond (I), a Formal Single Bond with a Phosphorous Cation and a Chalcogenide Anion (Zwitterionic Structure) (II), and a Hybrid (Intermediate) Resonance Form between I and II with a P−E Bond Order between 1 and 2 (III)

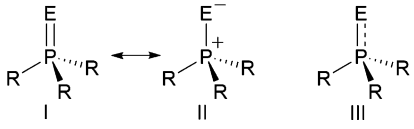

Substituent Effects. To see how resonance or inductive effects influence the strength of the P−E bond, we compared the bond dissociation ΔH(BDE) and Löwdin charges of *para*- and *meta*-monosubstituted (with NH_2−, MeO−, H−, F−, HO_2C−, and F− groups) triarylphosphine chalcogenides against known Hammett constants (σ_p or σ_m).[42] As shown in Figure 5, an increase in P−E bond strength, as measured by the ΔH(BDE), is accomplished by increasing the electron-donating ability of the *para* substituent, while the *meta* substituent has a smaller effect. However, both *para* and *meta* substituents have minor effects on the buildup of positive and negative Löwdin charges on P and chalcogen (E), respectively (Figure 6).

DOI: 10.1021/acs.organomet.5b00428
Organometallics 2015, 34, 4023−4031

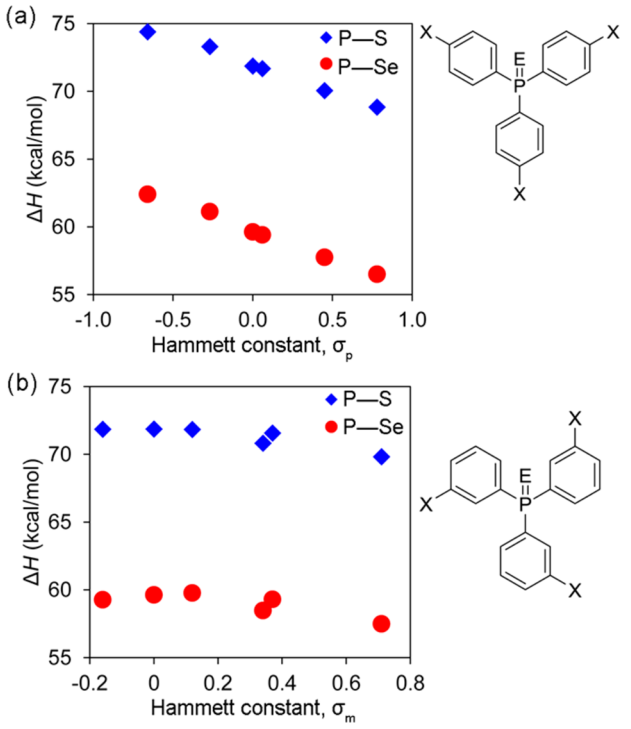

Figure 5. Calculated P−E bond dissociation ΔH(BDEs) vs Hammett constants in 4- (*para*) (a) and 3-substituted (*meta*) triarylphosphine chalcogenides (b).

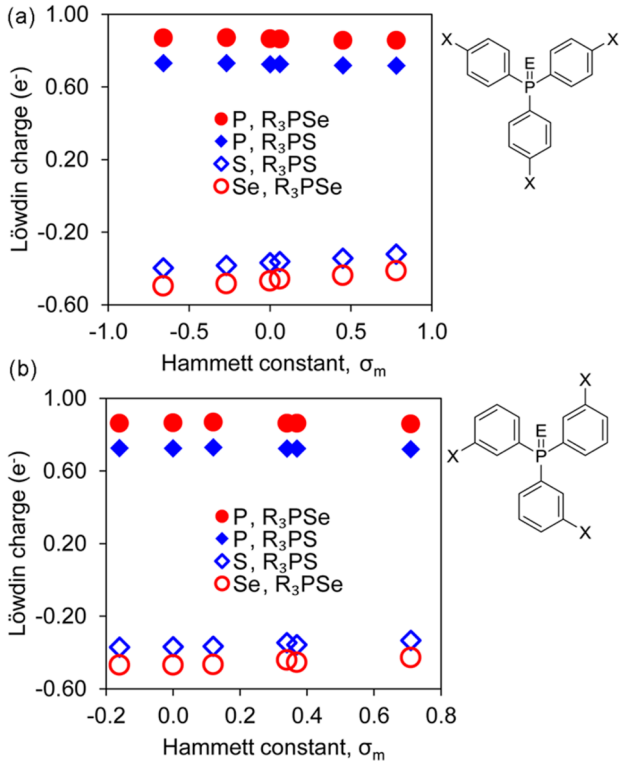

Figure 6. Calculated Löwdin charges on phosphorus and chalcogen atoms vs Hammett constants in 4- (*para*) (a) and 3-substituted (*meta*) (b) triarylphosphine chalcogenides.

Bond Order and Substituent Constants. To further examine the P−E bond in *para*- and *meta*-monosubstituted triarylphosphine chalcogenides, we calculated bond orders in GAMESS from the sum of the density matrices of the atoms in question, as described previously.[43−45] As could be expected based on simple atom size and orbital overlap considerations (see above), we find that the P−Se bond order (1.4−1.5) is generally lower than P−S bond order (1.7−1.8). For each chalcogenide family (sulfides or selenides), there is a stronger linear correlation between the P−E bond order and the identity of *para* substituents than that of the *meta* substituents (Figure 7). Increasing the electron-donating ability of the *para*

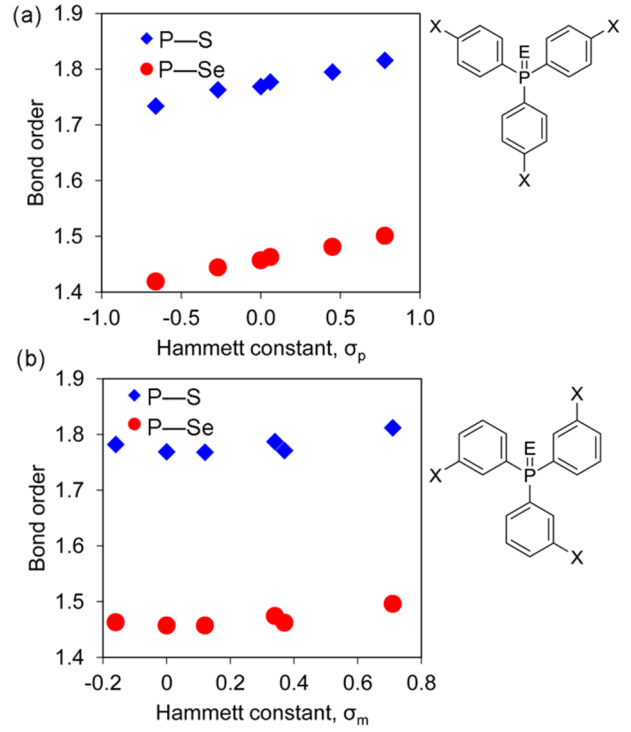

Figure 7. Calculated P−E bond order vs Hammett constants in 4- (*para*) (a) and 3-substituted (*meta*) (b) triarylphosphine chalcogenides.

substituent decreases the P−E bond order by up to ca. 0.1 (Figure 7a). This is consistent with the stronger electronic influence of substituents in the *para* and *ortho* positions compared to the *meta* position in organic chemistry. Thus, while bonding in the phosphine chalcogenides appears to have significant ionic character as noted above (Scheme 1), computational[24] and experimental studies show that a double-bond resonance structure (or at least partial multiple-bond character) is still important in rationalizing trends within closely related families of compounds such as *para*-monosubstituted triarylphosphine chalcogenides.

Correlating Experimental and Computational Results. Finally in this study, we sought to gain new insight into the predictive value of our calculations by investigating selected triarylphosphine compounds experimentally with ^{31}P and ^{77}Se spectroscopy (see Supporting Information for a complete table of NMR chemical shifts). The compounds we monitored by NMR include (2,4,6-MeO_3-C_6H_2)$_3$PE, (4-MeO-C_6H_4)$_3$PE, (4-F-C_6H_4)$_3$PE, and Ph_3PE; additionally, we added data from compounds we studied previously,[26] namely, $(PhO)_3$PE, $(Et_2N)_3$PE, (*n*-Pr)Ph_2PE, (*n*-Bu)$_3$PE, and (*n*-octyl)$_3$PE. Previously, the effect of substituents around P−E bonds on NMR spectra has been investigated in related arylphosphorothio-

DOI: 10.1021/acs.organomet.5b00428
Organometallics 2015, 34, 4023−4031

nates[46] and triarylselenophosphates.[47] The $^{31}P-^{77}Se$ coupling constant is also influenced by adjacent substituents.[48]

With multiple factors influencing the electron density on the P atom, it is not surprising to find out the scatter plot of all ^{31}P NMR chemical shifts (sulfides and selenides) and $^{1}J(^{31}P-^{77}Se)$ coupling constants (for selenides only) available to us does not show an immediate correlation with our calculated P−E bond dissociations, ΔH(BDEs) (Figure 8a). The lack of correlation between ^{31}P and P−E bond energy data is more generally a sign that bond angles and geometry, which vary widely among all the calculated structures, heavily impact ^{31}P chemical shifts. On the other hand, we find there is a very strong correlation between our experimentally measured ^{77}Se NMR chemical shifts and our calculated P−E bond dissociations, ΔH(BDEs), for the trisubstituted phosphine selenides (Figure 8b). More specifically, the ^{77}Se NMR chemical shifts move upfield and become more negative, as the P−Se ΔH(BDE) values increase. As mentioned above, a larger ΔH(BDE) value corresponds to a more polarized P−Se bond and a higher partial (Löwdin) negative charge on Se; this increase in electron density at Se helps explain the consequent and progressive upfield shift of the ^{77}Se resonances as the P−Se becomes stronger. We corroborated these experimental results with ^{77}Se NMR tensor calculations in Gaussian 03 using the optimized molecular geometries. There is a correlation between calculated NMR tensor and increasing ΔH(BDE). These results imply that increasing the electronic shielding around the Se nucleus leads to a stronger P−E bond with a stronger ionic character.

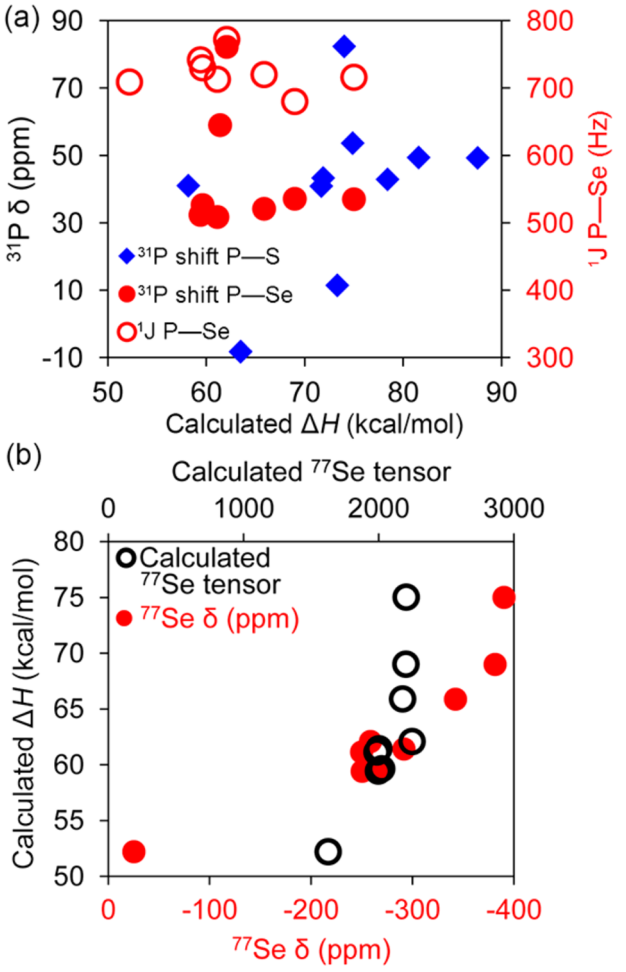

Figure 8. ^{31}P NMR chemical shifts and $^{1}J(^{31}P-^{77}Se)$ coupling constants vs calculated P−E ΔH(BDEs) of tertiary phosphine chalcogenides (a). ^{77}Se NMR chemical shifts and calculated ^{77}Se tensors vs calculated P−E ΔH(BDEs) of tertiary phosphine selenides.

CONCLUSIONS

We have investigated the bond strength and nature of bonding in multiple families of phosphine chalcogenide compounds. Generally, within a specific chalcogen family (sulfides or selenides), DFT computations show that the ΔH(BDE) increases as the P−E bond distance increases. This may be due to increasing partial positive and negative charges on the phosphorus and chalcogen atoms, respectively, which results in a stronger, slightly longer bond with greater ionic character. Monosubstituted triarylphosphine chalcogenides with electron-donating groups and negative Hammett constants exhibit stronger bonds, while the same class of compound with electron-withdrawing groups and positive Hammett constants exhibit weaker bonds. Electron-donating groups add electron density to the P−E unit, allowing for a bond of more ionic character by stabilization of the positive charge buildup on P. The net result of this effect is a P−E bond order between 1 and 2. We show that the computational results can be verified by ^{77}Se NMR spectroscopy, where more shielded nuclei having more negative ^{77}Se chemical shifts have stronger P−Se bonds as measured by higher ΔH(BDE) values. We anticipate that our results will allow for the design of new atom transfer and colloidal nanocrystal synthesis reagents and reactions with full reproducibility and enhanced utility.

COMPUTATIONAL AND EXPERIMENTAL METHODS

Computations. All calculations were carried out using GAMESS[49,50] (May 2013 version, revision 1) with DFT and the Tao−Perdew−Staroverov−Scuseria (TPSS)[51,52] functional. The accuracy of the new generation functional TPSS is known to match or exceed almost all prior functionals, including the popular hybrid functional B3LYP.[53] TPSS reproduces geometric properties at least as precisely as B3LYP and can recognize relatively weak interactions (such as agostic interactions), while B3LYP significantly underestimates them.[54] Since hydrogen atoms in the systems we modeled did not play significant roles, we used the 6-311G* basis set[55] for all elements. By not applying polarization functions on H atoms far from the phosphorus center, the calculations are accelerated considerably without significantly degrading computational precision or accuracy.[56] All structures were fully optimized and Hessian calculations (frequency analyses) were performed to ensure a minimum was achieved with zero imaginary vibrational frequencies. Thermodynamic functions, including enthalpies, entropies, and free energies, were calculated at 298.15 K and 1 atm. Results were visualized with MacMolPlt.[57] Calculations of NMR tensors were carried out using Gaussian 03[58] at the same level of theory as used above with the gauge-independent atomic orbital (GIAO) method.[59−63]

Materials. Unless otherwise noted, all chemicals were used as received without further purification. Triphenylphosphine (99%) was purchased from Acros; sulfur (99.999%), selenium (99.999%), and tris(4-fluorophenyl)phosphine (98%) were purchased from Alfa Aesar; tris(pentafluorophenyl)phosphine (98%), tris(4-methoxyphenyl)-phosphine (98%), and tris(2,4,6-trimethoxyphenyl)phosphine (98%) were from Strem; toluene (99.9%), xylenes (99.9%), and chloroform (99.9%) were from Fisher.

Characterization. ^{31}P NMR chemical shifts were referenced to 85% phosphoric acid, H_3PO_4 (δ 0 ppm). ^{77}Se NMR spectra were referenced to $Ph_3PSe/CDCl_3$ (δ 266.20 ppm vs Me_2Se δ 0 ppm).

DOI: 10.1021/acs.organomet.5b00428
Organometallics 2015, 34, 4023−4031

Synthesis. Triphenylphosphine selenide,[15] tris(4-fluorophenyl)-phosphine sulfide, tris(4-fluorophenyl)phosphine selenide, tris(2,4,6-trimethoxyphenyl)phosphine sulfide, and tris(2,4,6-trimethoxyphenyl)phosphine selenide[64] were prepared as described previously. Tris(pentafluorophenyl)phosphine sulfide was prepared with a modified procedure;[65−67] briefly, tris(pentafluorophenyl)phosphine (50.3 mg, 0.0945 mmol) and sulfur (2.8 mg, 0.0873 mmol) were heated to reflux in xylenes for 4 days. Solvent was removed under vacuum. The crude was recrystallized from ethanol to give white needles (29.5 mg, 60.1%). ^{31}P NMR: −8.28 ppm; ^{19}F NMR: 131.54 ppm (d, 22.20 Hz), 143.53 ppm (t, 21.07 Hz), 157.84 ppm (t, 20.89 Hz).

■ ASSOCIATED CONTENT

Supporting Information

The Supporting Information is available free of charge on the ACS Publications website at DOI: 10.1021/acs.organomet.5b00428.

Plots of calculated P−E distance and Löwdin charge against ΔH of bond dissociation for all compounds; tables of calculated geometric parameters and dissociation energies; tables of ^{31}P and ^{77}Se chemical shifts; Cartesian coordinates and absolute energies for all compounds (PDF)

XYZ file (XYZ)

■ AUTHOR INFORMATION

Corresponding Authors

*E-mail: hjfan@pvamu.edu.

*E-mail: vela@iastate.edu.

Notes

The authors declare no competing financial interest.

■ ACKNOWLEDGMENTS

J.V. gratefully acknowledges the National Science Foundation for funding of this work through the Division of Materials Research, Solid State and Materials Chemistry program (NSF-DMR-1309510). H.-J.F. thanks the Department of Chemistry at Prairie View A&M University for release time and a 2014 Summer Research mini-grant (115103-00011), and the U.S. Department of Energy, National Nuclear Security Administration, for support (DE-NA 0001861). S.R.A. thanks Stephen Todey for assistance with NMR experiments. The authors would like to dedicate this work to Prof. John Verkade for his six decades of research excellence and thank him, Pat Holland, Gordie Miller, and Arthur Winter for comments.

■ REFERENCES

(1) Davies, R. Chalcogen-Phosphorus (and Heavier Congeners) Chemistry. In *Handbook of Chalcogen Chemistry: New Perspectives in Sulfur, Selenium and Tellurium*; Devillanova, F. A., Ed.; Royal Society of Chemistry: Cambridge, 2007; pp 286−343.

(2) Donahue, J. P. *Chem. Rev.* **2006**, *106*, 4747−4783.

(3) Brown, D. H.; Cross, R. J.; Keat, R. *J. Chem. Soc., Dalton Trans.* **1980**, 871−874.

(4) Baechler, R. D.; Stack, M.; Stevenson, K.; Vanvalkenburgh, V. *Phosphorus, Sulfur Silicon Relat. Elem.* **1990**, *48*, 49−52.

(5) Kullberg, M.; Stawinski, J. *J. Organomet. Chem.* **2005**, *690*, 2571−2576.

(6) Aizawa, S.; Majumder, A.; Maeda, D.; Kitamura, A. *Chem. Lett.* **2009**, *38*, 18−19.

(7) Tsukuda, T.; Miyoshi, R.; Esumi, A.; Yamagiwa, A.; Dairiki, A.; Matsumoto, K.; Tsubomura, T. *Inorg. Chim. Acta* **2012**, *384*, 149−153.

(8) Bollmark, M.; Stawinski, J. A. *Chem. Commun.* **2001**, 771−772.

(9) McDonough, J. E.; Mendiratta, A.; Curley, J. J.; Fortman, G. C.; Fantasia, S.; Cummins, C. C.; Rybak-Akimova, E. V.; Nolan, S. P.; Hoff, C. D. *Inorg. Chem.* **2008**, *47*, 2133−2141.

(10) Murray, C. B.; Norris, D. J.; Bawendi, M. G. *J. Am. Chem. Soc.* **1993**, *115*, 8706−8715.

(11) García-Rodríguez, R.; Hendricks, M. P.; Cossairt, B. M.; Liu, H.; Owen, J. S. *Chem. Mater.* **2013**, *25*, 1233−1249.

(12) Sowers, K. L.; Swartz, B.; Krauss, T. D. *Chem. Mater.* **2013**, *25*, 1351−1362.

(13) Bullen, C. R.; Mulvaney, P. *Nano Lett.* **2004**, *4*, 2303−2307.

(14) Yang, P.; Tretiak, S.; Ivanov, S. *J. Cluster Sci.* **2011**, *22*, 405−431.

(15) Evans, C. M.; Evans, M. E.; Krauss, T. D. *J. Am. Chem. Soc.* **2010**, *132*, 10973−10975.

(16) Steckel, J. S.; Yen, B. K. H.; Oertel, D. C.; Bawendi, M. G. *J. Am. Chem. Soc.* **2006**, *128*, 13032−13033.

(17) Koh, W.-k.; Yoon, Y.; Murray, C. B. *Chem. Mater.* **2011**, *23*, 1825−1829.

(18) Liu, H.; Owen, J. S.; Alivisatos, A. P. *J. Am. Chem. Soc.* **2007**, *129*, 305−312.

(19) Gary, D. C.; Glassy, B. A.; Cossairt, B. M. *Chem. Mater.* **2014**, *26*, 1734−1744.

(20) Chernick, C. L.; Pedley, J. B.; Skinner, H. A. *J. Chem. Soc.* **1957**, 1851−1854.

(21) Capps, K. B.; Wixmerten, B.; Bauer, A.; Hoff, C. D. *Inorg. Chem.* **1998**, *37*, 2861−2864.

(22) Gilheany, D. G. *Chem. Rev.* **1994**, *94*, 1339−1374.

(23) Ibdah, A.; Espenson, J. A.; Jenks, W. S. *Inorg. Chem.* **2005**, *44*, 8426−8432.

(24) Sandblom, N.; Ziegler, T.; Chivers, T. *Can. J. Chem.* **1996**, *74*, 2363−2371.

(25) Dobado, J. A.; Martínez-García, H.; Molina, J.; Sundberg, M. R. *J. Am. Chem. Soc.* **1998**, *120*, 8461−8471.

(26) Ruberu, T. P. A.; Albright, H. R.; Callis, B.; Ward, B.; Cisneros, J.; Fan, H.-J.; Vela, J. *ACS Nano* **2012**, *6*, 5348−5359.

(27) Verkade, J. G.; Kisanga, P. B. *Tetrahedron* **2003**, *59*, 7819−7858.

(28) Guo, Y.; Alvarado, S. R.; Barclay, J. D.; Vela, J. *ACS Nano* **2013**, *7*, 3616−3626.

(29) Kaupp, M.; Metz, B.; Stoll, H. *Angew. Chem., Int. Ed.* **2000**, *39*, 4607−4609.

(30) Kaupp, M.; Riedel, S. *Inorg. Chim. Acta* **2004**, *357*, 1865−1872.

(31) Lindquist, B. A.; Dunning, T. H. *J. Phys. Chem. Lett.* **2013**, *4*, 3139−3143.

(32) Ernst, R. D.; Freeman, J. W.; Stahl, L.; Wilson, D. R.; Arif, A. M.; Nuber, B.; Ziegler, M. L. *J. Am. Chem. Soc.* **1995**, *117*, 5075−5081.

(33) Wada, M.; Higashizaki, S. *J. Chem. Soc., Chem. Commun.* **1984**, 482−483.

(34) *CRC Handbook of Chemistry and Physics*, 95th ed.; CRC Press: Boca Raton, FL, 2014−2015.

(35) Bautista, J. L.; Flores-Alamo, M.; Tiburcio, J.; Vieto, R.; Torrens, H. *Molecules* **2013**, *18*, 13111−13123.

(36) Wang, Y.; Parkin, S. R.; Gierschner, J.; Watson, M. D. *Org. Lett.* **2008**, *10*, 3307−3310.

(37) Mulliken, R. S. *J. Chem. Phys.* **1955**, *23*, 1833−1840.

(38) Mulliken, R. S. *J. Chem. Phys.* **1955**, *23*, 1841−1846.

(39) Mulliken, R. S. *J. Chem. Phys.* **1955**, *23*, 2338−2342.

(40) Mulliken, R. S. *J. Chem. Phys.* **1955**, *23*, 2343−2346.

(41) Löwdin, P.-O. *Adv. Chem. Phys.* **1970**, *5*, 185−199.

(42) Hansch, C.; Leo, A.; Taft, R. W. *Chem. Rev.* **1991**, *91*, 165−195.

(43) Giambiagi, M.; Giambiagi, M.; Grempel, D. R.; Heymann, C. D. *J. Chim. Phys. Phys.-Chim. Biol.* **1975**, *72*, 15−22.

(44) Mayer, I. *Chem. Phys. Lett.* **1983**, *97*, 270−274.

(45) Mayer, I. *Chem. Phys. Lett.* **1985**, *117*, 396.

(46) Hernández, J.; Goycoolea, F. M.; Zepeda-Rivera, D.; Juárez-Onofre, J.; Martínez; Lizardi, J.; Salas-Reyes, M.; Gordillo, B.; Velázquez-Contreras, C.; García-Barradas, O.; Cruz-Sánchez, S.; Domínquez, Z. *Tetrahedron* **2006**, *62*, 2520−2528.

(47) Domínguez, Z.; Hernández, J.; Silva-Gutiérrez, L.; Salas-Reyes, M.; Sánchez, M.; Merino, G. *Phosphorus, Sulfur Silicon Relat. Elem.* **2010**, *185*, 772−784.

DOI: 10.1021/acs.organomet.5b00428
Organometallics 2015, 34, 4023−4031

(48) Pinnell, R. P.; Megerle, C. A.; Manatt, S. L.; Kroon, P. A. *J. Am. Chem. Soc.* **1973**, *95*, 977−978.
(49) Schmidt, M. W.; Baldridge, K. K.; Boatz, J. A.; Elbert, S. T.; Gordon, M. S.; Jensen, J. S.; Koseki, S.; Matsunaga, N.; Nguyen, K. A.; Su, S.; Windus, T. L.; Dupuis, M.; Montgomery, J. A. *J. Comput. Chem.* **1993**, *14*, 1347−1363.
(50) Gordon, M. S.; Schmidt, M. W. Advances in Electronic Structure Theory: GAMESS a Decade Later. In *Theory and Applications of Computational Chemistry: The First Forty Years*; Dykstra, C. E., Frenking, G., Kim, K. S., Scuseria, G. E., Eds.; Elsevier Science: Amsterdam, 2005; p 1167.
(51) Perdew, J. P.; Tao, J.; Staroverov, V. N.; Scuseria, G. E. *Phys. Rev. Lett.* **2003**, *91*, 146401.
(52) Perdew, J. P.; Tao, J.; Staroverov, V. N.; Scuseria, G. E. *J. Chem. Phys.* **2004**, *120*, 6898−6911.
(53) Staroverov, V. N.; Scuseria, G. E.; Tao, J. M.; Perdew, J. P. *J. Chem. Phys.* **2003**, *119*, 12129−12137.
(54) Fan, Y.; Bacon, S.; Kolade, A.; Wasiu, A.; Fan, H.-J. ICCS: A DFT Study on the Mechanism of Wolff Rearrangement in a Five-member Iridacycle. *ICCS 2010 - International Conference on Computational Science, Proceedings* **2010**, *1*, 2653−2661.
(55) Krishnan, R.; Binkley, J. S.; Seeger, R.; Pople, J. A. *J. Chem. Phys.* **1980**, *72*, 650−654.
(56) Fan, Y. B.; Hall, M. B. *Organometallics* **2005**, *24*, 3827−3835.
(57) Bode, B. M.; Gordon, M. S. *J. Mol. Graphics Modell.* **1998**, *16*, 133−138.
(58) Frisch, M. J.; Trucks, G. W.; Schlegel, H. B.; Scuseria, G. E.; Robb, M. A.; Cheeseman, J. R.; Montgomery, J. A.; Vreven, T.; Kudin, K. N.; Burant, J. C.; et al. *Gaussian 03* revision D.01; Gaussian, Inc.: Wallingford, CT, 2004.
(59) London, F. The quantic theory of inter-atomic currents in aromatic combinations. *J. Phys. Radium* **1937**, *8*, 397−409.
(60) McWeeny, R. Perturbation Theory for Fock-Dirac Density Matrix. *Phys. Rev.* **1962**, *126*, 1028.
(61) Ditchfield, R. Self-consistent perturbation theory of diamagnetism. 1. Gauge-invariant LCAO method for N.M.R. chemical shifts. *Mol. Phys.* **1974**, *27*, 789−807.
(62) Wolinski, K.; Hilton, J. F.; Pulay, P. Efficient Implementation of the Gauge-Independent Atomic Orbital Method for NMR Chemical Shift Calculations. *J. Am. Chem. Soc.* **1990**, *112*, 8251−8260.
(63) Cheeseman, J. R.; Trucks, G. W.; Keith, T. A.; Frisch, M. J. A Comparison of Models for Calculating Nuclear Magnetic Resonance Shielding Tensors. *J. Chem. Phys.* **1996**, *104*, 5497−5509.
(64) Wada, M.; Kanzaki, M.; Fujiwara, M.; Kajihara, K.; Erabi, T. *Bull. Chem. Soc. Jpn.* **1991**, *64*, 1782−1786.
(65) Burdon, J.; Rozhkov, I. N.; Perry, G. M. *J. Chem. Soc. C* **1969**, 2615−2617.
(66) Emeléus, H. J.; Miller, J. M. *J. Inorg. Nucl. Chem.* **1966**, *28*, 662−665.
(67) Miller, J. M. *J. Chem. Soc. A* **1967**, 828−834.

DOI: 10.1021/acs.organomet.5b00428
Organometallics 2015, 34, 4023−4031